JOURNAL OF MATERIALS SCIENCE 26 (1991) 4697–4701

Microstructure and strength of Si–Ti–C–O, fibre-reinforced aluminium and aluminium alloys

T. B. WILLIAMS*, D. SHINDO, E. AOYAGI, M. HIRABAYASHI‡
Institute for Materials Research, Tohoku University, 2-1-1 Katahira, Sendai 980, Japan
Y. WAKU, M. SUZUKI
Ube Industries, Ltd., Ube City, Yamaguchi Prefecture, Japan

Microstructures of Si–Ti–C–O fibre-reinforced aluminium and aluminium alloys were investigated by scanning electron microscopy, and both conventional and analytical transmission electron microscopy. In the latter samples, some inclusions were observed between the matrix and the fibres. From the electron diffraction, high resolution microscopy and compositional analysis by energy-dispersive X-ray, the inclusions were identified as the α-Al–Si–Fe phase. Since the longitudinal three-point bending strength decreases with the increase of iron content, it was concluded that the α-phase inclusions on the surface of the fibre contribute to the lower strength of the composites based on this alloy.

1. Introduction

There has recently been much interest in the development of composite materials which combine the physical properties of a metallic matrix and those of ceramic powders, whiskers or fibres. The resulting composites offer a performance which combines those of the matrix and reinforcing phases. Industries which have traditionally sought high performance from fabrication materials under extreme conditions, such as the aerospace, defence and more recently the automotive industries would be those most likely to benefit from the ready availability of such materials. Hence considerable effort has been put into the development of composites based on the commonly used light-weight aluminium alloys which form the major part of, for example, traditionally constructed aircraft frames. In other industries, the replacement of components presently cast from iron-based alloys with alternatives produced from an aluminium-based composite would have considerable advantages both in fabrication, due to the lower cost of aluminium squeeze casting methods over those for higher melting-point metals and as lighter, more corrosion-resistant end-products.

Although aluminium alloys have useful strength-to-weight ratios at normal temperatures, their performance invariably deteriorates dramatically at elevated temperatures, with the upper limits typically well below 300 °C. This is particularly true with precipitation-hardened alloys as extended high-temperature use causes 'over-ageing' by growth of the finely-dispersed hardening precipitates. Hence, the availability of a low-cost and relatively temperature-indepèndent hardening method would have considerable impact in many areas. As fuel economy becomes an increasingly more important criterion in the design of internal combustion engines, resulting in a need for lighter construction materials and more efficient engines, the fabrication of reciprocating pistons and valves which are directly subject to combustion gases may be a future application. Considerable advantages, particularly in reciprocating engine components, might be expected from lighter fibre–alloy or fibre–whisker composites.

The development of metal-based composites has in some respects paralleled that in the plastics industry, with the morphologies of the ceramic or metallic inclusions varying from those of powders, through short single-crystal or 'whisker' particles to extended fibre reinforcement. It is the latter method with which we are concerned in this paper.

Recently, the potential of a new continuous Si–Ti–C–O fibre (Tyranno-fibre®) for reinforcement of a pure Al matrix (Japan Industrial Standard (JIS) 1070) and Al–Ni alloy has been discussed [1–3]. This fibre offers a better thermal performance than alternatives such as C (carbon fibre), SiC or SiC/C fibres, and furthermore the high knot-strength [1] allows the

® Tyranno fibre is a trademark of Ube Industries, Ltd.

Present address: CSIRO Division of Materials Science and Technology, Locked Bag 33, Clayton, 3168 Victoria, Australia.
‡*Present address*: Kitami Institute of Technology, Kitami 090, Japan.

0022–2461/91 $03.00 + .12

TABLE I Chemical composition of alloys

Sample No.	Cu	Si	Fe	Mn	Mg	Zn	Ti	Cr	Al (wt %)
Typical "pure" aluminium ingots									
	0.0	0.02	0.10	0.0	0.0	0.0	0.0	0.0	balance
Typical commercial 6061 ingot, as-supplied									
	0.25	0.65	0.28	0.04	0.91	0.11	–	0.08	balance
Modified 6061 ingots with varying Fe contents									
1	0.203	0.701	0.024	0.003	0.960	0.001	–	0.068	balance
2	0.205	0.686	0.122	0.007	0.978	0.001	–	0.068	balance
3	0.194	0.732	0.411	0.006	0.982	0.007	–	0.074	balance
4	0.185	0.726	0.583	0.005	0.955	0.007	–	0.074	balance
5	0.182	0.718	0.769	0.006	0.938	0.007	–	0.071	balance

pre-formation of complex woven shapes for introduction into the aluminium melt. Tensile strengths of the order of 1 GPa at room temperature after heat treatment at 400 °C for periods up to 400 h were reported for these composites. However, the general utility of this material as a commercially viable reinforcing fibre requires that a similarly high performance be obtained using matrices of the more common and lower-cost aluminium-based alloys, which typically contain appreciable quantities of other elements (see Table I), and the matrix microstructure then becomes an additional and important consideration.

We report here the results of a study by scanning electron microscopy (SEM) and both conventional and analytical transmission electron microscopy (TEM/AEM) of a commercial alloy (6061) and of similar alloys containing slightly different amounts of iron, reinforced with continuous Si–Ti–C–O fibre. The effect of the matrix microstructure on the resulting mechanical properties is discussed. The effects of intentionally varying other minor constituents of the 6061 alloy besides iron are currently being investigated and will be reported later.

2. Experimental procedure

2.1. Casting procedure

Samples of pure aluminium (JIS 1070) and alloys (JIS 6061, and 6061 with varying amounts of added Fe) were cast with ~ 55% volume Si–Ti–C–O fibre having SiC powder (with average particle diameters ~ 0.27 μm) attached to its surface, in the form of rods and billets of about 1–2 cm^2 in cross-section at Ube Industries, Ltd, Yamaguchi Prefecture, Japan. The fibre preforms of about 55% volume arranged unidirectionally were pre-heated to 650 °C and introduced into a melt held at 700 °C. The particles prevent the fibres from touching and allow the melt to flow between them. A casting (extrusion) pressure of 1000 kg cm^{-2} was used for all the samples examined. In order to examine the effect of the majority impurity phases present in the 6061 alloy, mixtures of pure aluminium with varying and controlled amounts of added elemental impurities were prepared and samples were cast from these alloys. Only the results of the variation in Fe content will be considered in this report. All the castings were analysed by conventional chemical methods, summarized in Table I.

2.2. Mechanical testing and microscopic examination

Both longitudinal and transverse (relative to fibre direction) three-point flexural-strength tests were performed using as-cast samples at room temperature. Strength tests on heat-treated samples are in progress and the results will be published later. Cross-sectioned and polished surfaces of all the samples were examined by Hitachi S800 SEM using both secondary and backscattered electron imaging. TEM samples were prepared by argon-ion beam etching polished sections of ~ 20 μm thick to electron transparency. They were examined in Jeol 2000 FX AEM and Jeol 2000 EX and 200 CX conventional TEMs. For the AEM examination, Tracor–Northern energy-dispersive X-ray (EDX) analysis equipment was used with the supplied factory software 'MICROQ' for data reduction, and reliable reference materials were employed for standardization.

3. Results and discussion

3.1. Mechanical testing

The results of the mechanical tests on the pure aluminium, 6061 alloy and modified 6061-like alloy samples are given in Table II, and those for the variation in Fe content of the latter are summarized graphically in Fig. 1. The pure aluminium matrix gave the highest mechanical strength in longitudinal flexural tests, with strengths similar to those previously reported [1]. The initial results of varying the Fe content of the matrix suggested that the Fe present in 6061 may contribute in part to the lower strength of composites based on this alloy.

3.2. SEM examination

Fig. 2a–d shows selected SEM images from polished cross-sections of the 6061-based composite. The SiC powder particles are clearly visible as black dots in Fig. 2a and irregular particles (P) in the remaining

TABLE II Mechanical test results for composites

No.	Fe (wt %)	Flexural strength at room temperature: Mean transverse (GPa)	Mean longitudinal (GPa)
Pure aluminium matrix			
	0.11	0.266	1.376
Modified 6061 matrices			
1	0.024	0.359	0.927
2	0.122	0.344	0.831
3	0.411	0.282	0.617
4	0.583	0.336	0.573
5	0.769	0.343	0.613

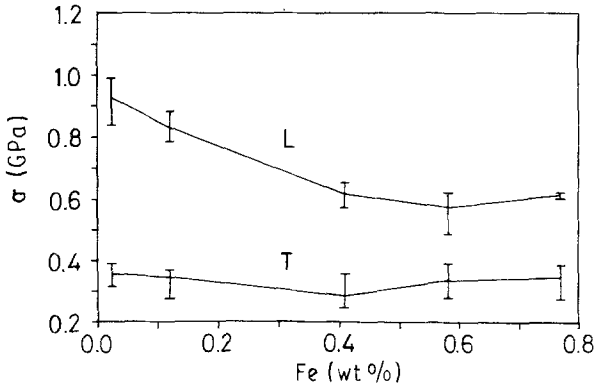

Figure 1 Variation of transverse (T) and longitudinal (L) three-point bending strength with Fe content, in various modified 6061 + fibre composites.

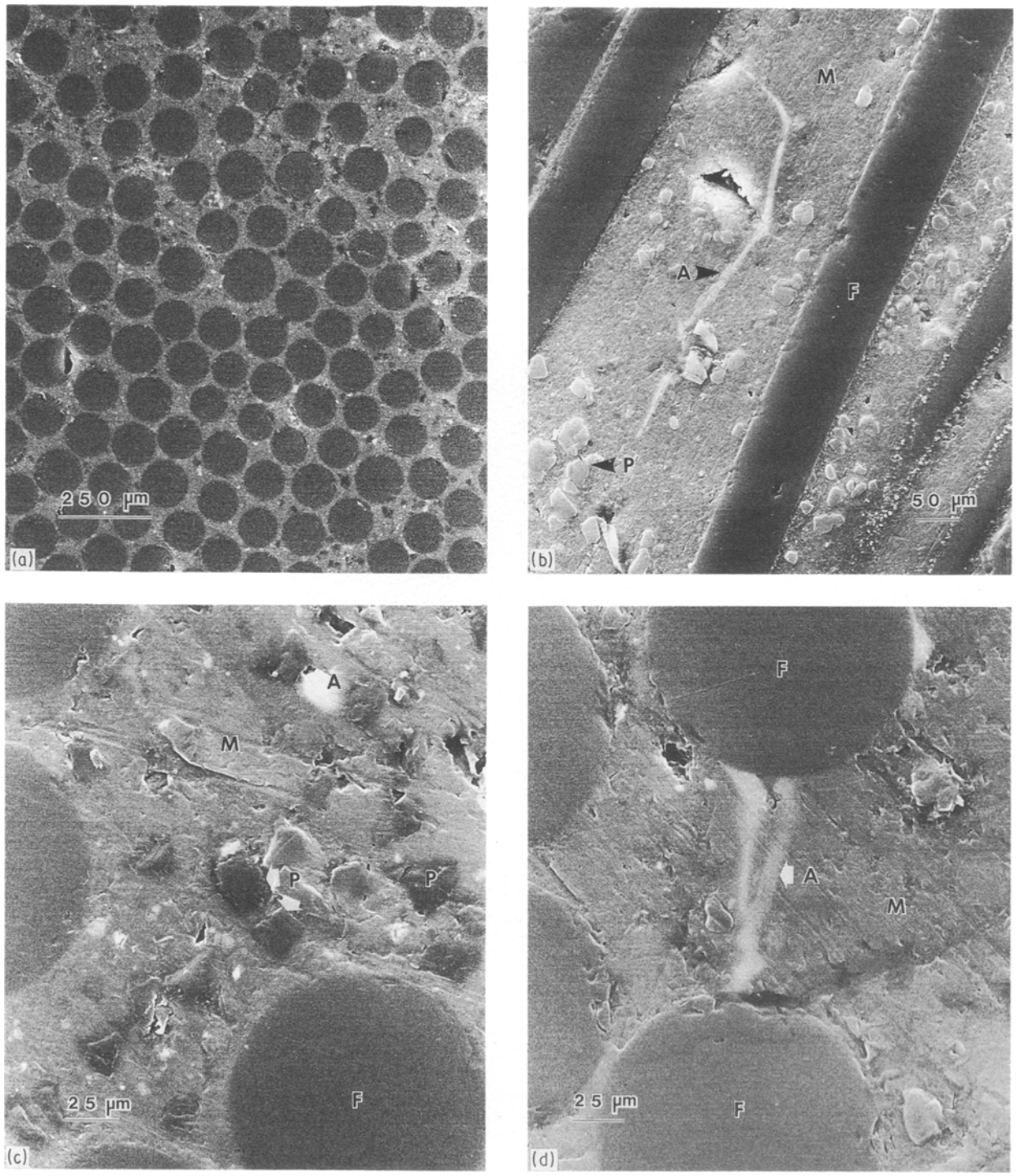

Figure 2 (a–d) SEM images (secondary electrons) of 6061 + fibre composites. (b) Longitudinal section, the remainder are transverse. Matrix (M), fibres (F), SiC powder (P) and inclusion particles (A) are indicated.

images. Also observed in the images from the alloy-matrix samples but not in those based on pure Al were small inclusions or precipitates (A); bright contrast in back-scattered images indicated a higher average atomic number than the matrix. These particles were found at both matrix grain boundaries (Fig. 2b) and at the fibre–matrix interface (Fig. 2d), and in some cases there is visual evidence that the fibres may have nucleated these particles. To test this, samples of 6061 stock alloy were cast without the fibre or SiC powder addition. Here also, the precipitates were observed in similar amounts and with similar morphologies to the composite samples, but it is not possible to completely rule out nucleation by the fibres.

3.3. TEM examination

In relatively low magnification TEM images, irregular (Fig. 3a) and occasionally needle-like (Fig. 3b) metallic inclusion particles were observed. From several such particles, a series of electron diffraction patterns was obtained by tilting the particles around dense reciprocal-space rows in order to determine the unit cell by the usual geometrical construction method. A cubic body-centered (b c c) unit cell with $a = 1.256$ nm was deduced. A many-beam lattice image from the [0 0 1] zone was obtained from one particle, shown in Fig. 4 together with the corresponding electron diffraction pattern (a) and a calculated image (b) from the b c c α-Al–Si–(Mn, Fe) structure [4, 5]. The cell deduced for these particles is in agreement with the data of Liu *et al.* [6], who observed the α-phase (and also several new binary and ternary compounds) in alloys of similar composition to those examined here, obtaining the same value for the cubic-cell constant from their electron diffraction results. This place was also observed in the age-hardening 6010 alloy [7] and in an Al–0.25 wt % Fe–0.13 wt % Si alloy [8].

3.4. AEM analysis

Using only regions which projected clear of the matrix and Si–Ti–C–O fibre regions (see for example Fig. 3b), EDX analyses were obtained for four such particles. These results are given numerically in Table III, with a representative EDX spectrum shown in Fig. 5. The inclusion particles always contained Al, Fe and Si, occasionally with rather lower quantities of Cr and Cu. Although Cu was also present to some degree as a background in these analyses, this was always much lower than the amount observed in the particle analysis. Data reduction was not performed for the minority elements, the data of Table III assuming that the sum of (Al + Fe + Si) for the particles was 100%. The averaged analyses for these particles suggest a composition of $\sim Al_9Fe_{2.25}Si_{1.46}$, close to the stoichiometry $Al_9Mn_2Si_{1.8}$ reported for α-(Al–Si–Mn) (and probably the iso-structural iron-containing variant also) [4]. These particles thus appear to be the b c c α-phase. Formation of the hexagonal α-phase of the same approximate composition as the cubic one is apparently prevented by the presence of rather small amounts of other metals such as Mn and Cr [9], which certainly occur in the 6061 alloy in sufficient quantities. The phases occurring in dilute Fe and Si-containing squeeze casting alloys have recently been examined in detail [8]; a majority of the cubic α-Al–Fe–Si phase was also found in this study. Our results here are in full agreement with the earlier findings. According to the structure determination [4,

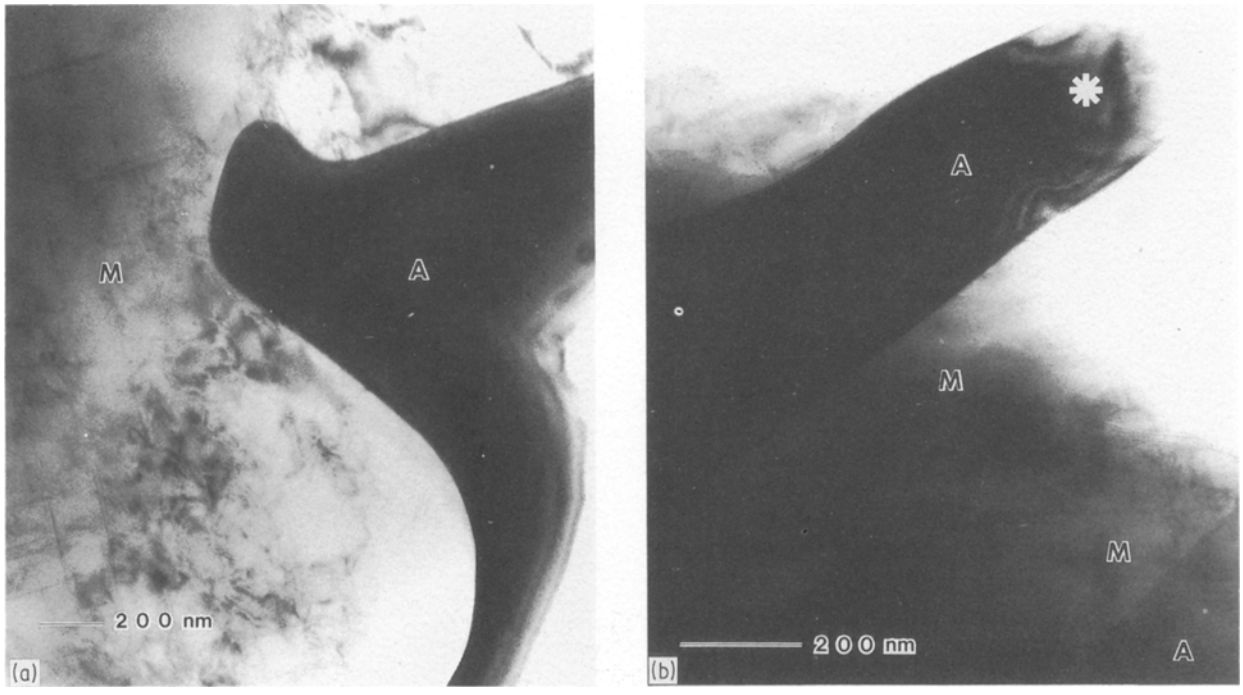

Figure 3 (a, b) Low-magnification TEM images of inclusion particles (dark regions, marked A) in the 6061 matrix (M). (a) Numerous dislocations are visible which do not appear to penetrate the inclusion particles. The particle A in (b) was analysed by EDX at the point marked with a star.

TABLE III EDX analysis of inclusion particles

Analysis	Si	Fe	Al	Total (wt %)
1	9.92	30.33	59.74	99.99
2	10.14	29.35	60.50	99.99
3	10.21	31.51	58.27	99.99
4	8.28	32.86	58.84	99.98
Mean	9.64	31.01	59.34	—
Atomic ratios	1.46	2.25	9.0	—

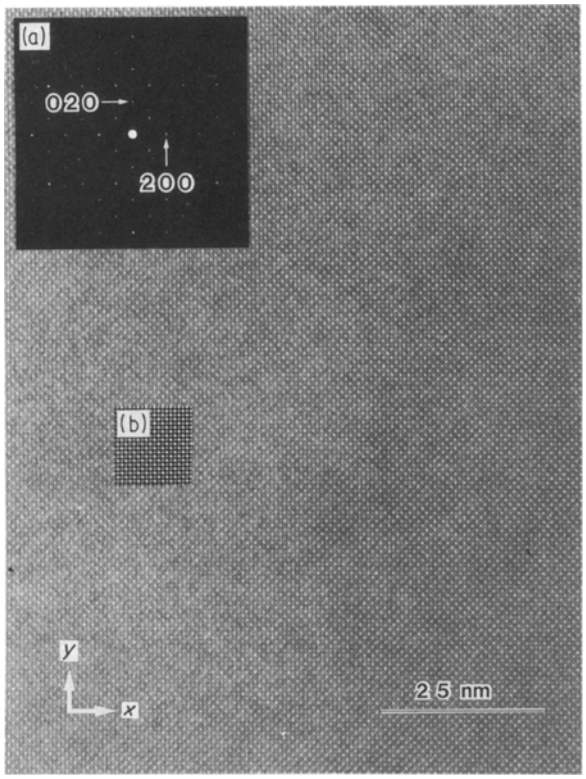

Figure 4 TEM image of an α-phase inclusion parallel with the [0 0 1] axis with (inset) zone-axis diffraction pattern (a) and simulated α-phase image (b) from a foil 12 nm thick. Absent reflections in the diffraction pattern are consistent with the body-centring.

5] there is some vacancy in atom-site occupation, and that work also did not distinguish between Al and Si atoms, which may account for the slight differences between our composition and that reported earlier.

4. Conclusions

Whilst the range of test strength against composition does not show a large variation with the iron content, the best performance was obtained with the lowest iron level, suggesting that control over the iron level in the melt (and possibly those of other transition metals, such as manganese and chromium) will lead to greater reliability of the cast composite. As no other particles were observed at even very high magnifications in the TEM study, we conclude that the majority of the insoluble metallic constituents in the melt are consumed in the formation of the α-phase particles. A more likely loss of strength in these composites might

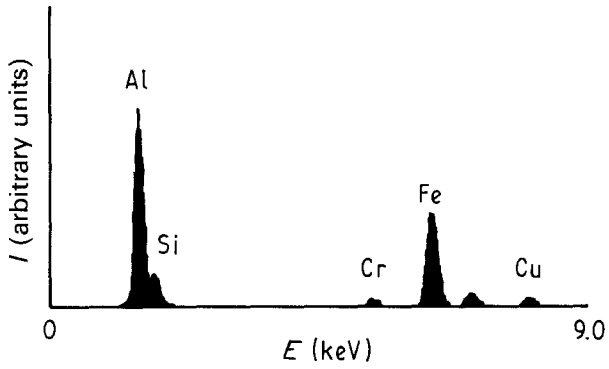

Figure 5 Representative AEM EDX analysis of an α-phase inclusion particle from the 6061 matrix, as collected. Intensity (I) in arbitrary units.

be the loss of plastic flow of the matrix and stress concentration by the presence of the harder particles, and this is supported in some degree by the image in Fig. 3a, in which the (darker) α particle is seen to be surrounded by dislocations which do not appear to penetrate it. It is also difficult to draw any conclusions from the transverse flexural strength against Fe content results as the strength here is much lower than longitudinally and controlled more by the fibre–matrix adhesion than the matrix ductility. Further work is currently in progress on these materials to explore the effect of the other metallic matrix constituents on the composite strength.

Acknowledgements

The authors wish to thank Professor K. Hiraga, Research Institute for Materials Research, Tohoku University for useful discussion. They also thank Mr T. Sakurai, Research Institute for Scientific Measurements, Tohoku University for his assistance during SEM observations. T. B. W. wishes to thank the Japan Society for the Promotion of Science for a supporting grant. We acknowledge the financial support of a grant-in-aid from the Japanese Ministry for Education Science and Culture.

References

1. T. YAMAMURA, Y. WAKU, T. YAMAMOTO, M. SHIBUYA, M. SUZUKI, T. HISHI and T. NAGASAWA, in "Looking ahead for Materials and Processes" (Elsevier, Amsterdam, 1987) p. 19.
2. Y. WAKU, T. YAMAMOTO, M. SUZUKI, T. NAGASAWA and T. NISHI, *Tetsu-to-Hagane* **75** (1989) 1563.
3. Y. WAKU, T. YAMAMOTO, M. SUZUKI, M. TOKUSE, T. NAGASAWA and T. NISHI, in Proceedings of the 34th International SAMPE Symposium and Exhibition (1989) 2278.
4. M. COOPER and K. ROBINSON, *Acta Cryst.* **20** (1966) 614.
5. M. COOPER, *ibid.* **23** (1967) 1106.
6. P. LIU, T. THORVALDSSON, G. L. DUNLOP, *Mater. Sci. Tech.* **2** (1986) 1009.
7. P. HODGSON and B. A. PARKER, *J. Mater. Sci.* **16** (1981) 1343.
8. P. SKJERPE, *Met. Trans.* **18A** (1987) 189.
9. D. MUNSON, *J. Inst. Met.* **95** (1967) 217.

Received 26 March
and accepted 20 December 1990